Controlling spatiotemporal chaos in the scenario of the one-dimensional Complex Ginzburg-Landau equation

BY S. BOCCALETTI[1] AND J. BRAGARD[2]

[1] *Istituto Nazionale di Ottica Applicata, Largo E. Fermi, 6,I-50125 Florence, Italy.*
[2] *Dept. of Physics and Applied Math, Universidad de Navarra, Irunlarrea s/n,E-31080 Pamplona, Spain*

We discuss some issues related with the process of controlling space-time chaotic states in the one dimensional Complex Ginzburg-Landau equation (CGLE). We address the problem of gathering control over turbulent regimes with the only use of a limited number of controllers, each one of them implementing in parallel a local control technique for restoring an unstable plane wave solution. We show that the system extension does not influence the density of controllers needed in order to achieve control.

Keywords: Chaos control, Complex Ginzburg-Landau equation.

1. Introduction

At first glance, controlling chaos may sound like an antinomy: one can find it difficult to understand how the concept of control could be applied to the concept of chaos. In fact, a huge literature of the nineties in the physics community has proved that these two terms can be reconciled, by showing that tiny perturbations applied to a chaotic system are sufficient to control its dynamics, driving it toward a desired target behavior.

The problem can be stated as follows: given a system (or a model equation representing to a good accuracy the dynamics of a specific process), how can one impose that such system performs a pre-determined operation? When the dynamical system is inherently chaotic, two options are possible. One can select parameters so as to drive back the system to a region where the dynamics is restored to a regular dynamics, and this process is usually referred to as suppression of chaos. Alternatively, one can take advantage of the great richness in the structure of the chaotic attractor, where infinite unstable periodic solutions are embedded. In this second case, usually referred to as control of chaos (Boccaletti *et al.*, 2000), one can properly select very tiny (in some case vanishingly small) perturbations able to force the appearance of a specific periodic behavior or a desired portion of the chaotic trajectory. Historically, the control of chaos grew as a more and more popular discipline as soon as scientists became aware of the omnipresence of chaos in dynamical systems.

The number of articles devoted to control of chaos experienced a huge grow in the scientific literature at the beginning of the nineties. After the seminal work by Ott-Grebogi-Yorke (OGY) (1990), there has been an everlasting interest in the control of chaos, and many alternative approaches have been suggested, as the time-delayed control method (Pyragas, 1992), and the adaptive method (Boccaletti & Arecchi, 1995). Furthermore, chaos control was theoretically proved in a large variety of time discrete, as well as time continuous systems (Boccaletti *et al.*, 2000) and even in the case of delayed dynamical systems (Boccaletti *et al.*, 1997).

The large body of literature devoted to this subject is rooted in the crucial role that chaos control can play in many practical applications, such as communications with chaos (Hayes *et al.* 1994), secure communication processes (Cuomo & Oppenheim 1993, Gershenfeld & Grinstein 1995, Kocarev & Parlitz 1995, Peng *et al.* 1996, Boccaletti *et al.* 1997b). Furthermore, experimental control of chaos has been achieved in many different areas such as chemistry (Petrov *et al.*, 1993), laser physics (Roy *et al.* 1992, Meucci *et al.* 1994, Meucci *et al.* 1996), electronic circuits (Hunt, 1991), and mechanical systems (Ditto *et al.*, 1990).

More recently, the interest switched to the application of control schemes in spatially extended systems. After some preliminary attempts (Aranson *et al.*, 1994) to control spatio-temporal chaos, attention has turned to the control of two-dimensional patterns (Lu *et al.* 1996, Martin *et al.* 1996), or of coupled map lattices (Parmananda *et al.* 1997, Grigoriev *et al.* 1997), or of particular model equations, such as the Complex Ginzburg-Landau equation (CGLE) (Montagne & Colet, 1997) and the Swift-Hohenberg equation for lasers (Bleich *et al.* 1992, Hochheiser *et al.* 1992).

While for time chaotic systems the different proposed schemes for chaos control have found several experimental verifications, in the extended case experimental realizations are so far limited in the field of nonlinear optics (Juul-Jensen *et al.* 1998, Benkler *et al.* 2000, Pastur *et al.* 2004) and also in the control of Kármán vortex street in two dimensional simulations of fluid turbulence (Patnaik & Wei, 2002). The main reason for this substantial lack of experimental verifications is that not all the proposed schemes for control of spatiotemporal chaos are straightforwardly implementable. For instance, many methods use space-extended perturbations, i.e. perturbations that have to be applied at any point of the system, and this requirement represents a serious limitation for any experimental implementations. In coupled map lattices, few examples of global control (Parmananda *et al.*, 1997), or control with a finite number of local perturbations (Grigoriev *et al.*, 1997) have been reported.

The most relevant question that arises when considering spatially extended systems is therefore to assess whether the perturbation itself should be extended in space, i.e. it must be applied to all points of the considered system. In this paper, we review some results about conditions for controlling chaos in spatially extended systems (Boccaletti *et al.*, 1999), with reference to the Complex Ginzburg-Landau Equation (CGLE). In the first two sections, after recalling the basic properties of CGLE, we will show that it is not necessary to apply control to all points of the systems, but we can rely on a finite number of local controllers. We will answer some questions about the cost of controlling a space extended system, and the time one has to wait in order to restore a regular dynamics from a chaotic one. Furthermore we will address issues such as which is the minimal number of local controllers that still provides control over the dynamics, and how strong the applied forcing must be in order to drive the system to a regular behavior. In the third section, we will show the results of using a parallel extension of the Pyragas' technique (Pyragas, 1992). The conclusive section overviews some still open problems.

2. The dynamical model

In the rest of this paper, we will test control schemes over the one-dimensional Complex Ginzburg-Landau equation (CGLE). This equation has been extensively investigated in the context of space-time chaos, since it describes the universal dynamical features of an extended system close to a Hopf bifurcation (Cross & Hohenberg 1993, Aranson & Kramer 2002), and therefore it can be considered as a good model equation in many different physical situations, such as in laser physics (Coullet *et al.*, 1989), fluid dynamics (Kolodner *et al.*, 1995), chemical turbulence (Kuramoto & Koga, 1981), bluff body wakes (Leweke & Provansal, 1994), or arrays of Josephson's junctions (Josephson, 1962).

In CGLE, a complex field $A(x,t) = \rho(x,t)e^{i\phi(x,t)}$ of modulus $\rho(x,t)$ and phase $\phi(x,t)$ obeys

$$\dot{A} \quad = \quad A + (1+i\alpha)\partial_x^2 A - (1+i\beta) \mid A \mid^2 A. \tag{2.1}$$

Here, dot denotes temporal derivative, ∂_x^2 stays for the second derivative with respect to the space variable $0 \leq x \leq L$ (L being the system extension), α and β are real coefficients characterizing linear and nonlinear dispersion. This model equation arises in physics as an "amplitude" equation, providing a reduced universal description of weakly nonlinear spatio-temporal phenomena in extended continuous media in the proximity of an Hopf bifurcation (Aranson & Kramer, 2002).

Different dynamical regimes occur in Eqs. (2.1) for different choices of the parameters α, β (Shraiman *et al.* 1992, Chate 1994).

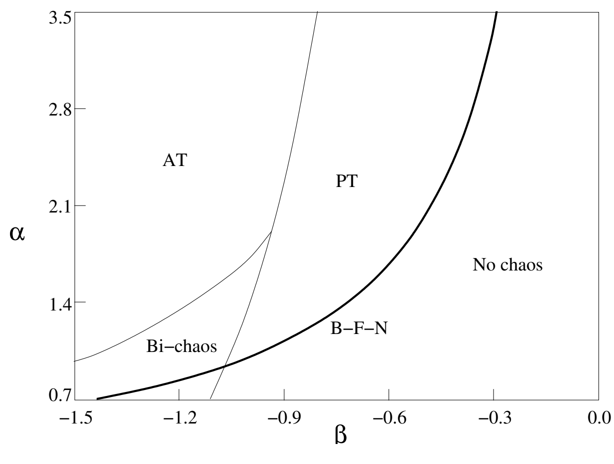

Figure 1. (α,β) parameter space for Eqs. (2.1). The lines delimit the borders for each one of the dynamical regimes produced by Eqs. (2.1), and the Benjamin-Feir-Newel (B-F-N) line for stability of the plane wave solutions. Amplitude Turbulence (AT) and Phase Turbulence (PT) are the main dynamical regimes of the CGLE (see text for their detailed description).

In particular, Eqs. (2.1) admits plane wave solutions (PWS) of the form

$$A_q(x,t) = \sqrt{1-q^2}\mathrm{e}^{\mathrm{i}(qx+\omega t)} \qquad -1 \leq q \leq 1. \tag{2.2}$$

Here, q is the wavenumber in Fourier space, and the temporal frequency is given by

$$\omega = -\beta - (\alpha - \beta)q^2. \tag{2.3}$$

The stability of such PWS can be analytically studied below the Benjamin-Feir-Newel (BFN) line (defined by $\alpha\beta = -1$ in the parameter space). Namely, for $\alpha\beta > -1$, one can define a critical wavenumber

$$q_c = \sqrt{\frac{1 + \alpha\beta}{2(1 + \beta^2) + 1 + \alpha\beta}} \tag{2.4}$$

such that all PWS are linearly stable in the range $-q_c \le q \le q_c$. Outside this range, PWS become unstable through the Eckhaus instability (Janiaud *et al.*, 1992).

When crossing from below the BFN line in the parameter space, Eq. (2.4) shows that q_c vanishes and all PWS become unstable. Above this line, one can identify different turbulent regimes (Shraiman *et al.* 1992, Chate 1994), called respectively Amplitude Turbulence (AT) or Defect Turbulence, Phase Turbulence (PT), Bi-chaos, and a Spatiotemporal Intermittent regime. The borders in parameter space for each one of these dynamical regimes are schematically drawn in Fig. 1, together with the BFN line. Along this review, we will concentrate on PT and AT, since they constitute the fundamental dynamical states of the fields, and their main properties have received considerable attention in recent years including the definition of suitable order parameters marking the transition between them (Torcini 1996, Torcini *et al.* 1997, Brusch *et al.* 2001).

Phase turbulence (PT) is a regime where the chaotic behavior of the field is dominated by the dynamics of $\phi(x, t)$. In PT the modulus $\rho(x, t)$ changes only smoothly, and is always bounded away from zero. At variance, AT is the dynamical regime wherein the fluctuations of $\rho(x, t)$ become dominant over the phase dynamics. The complex field experiences therefore large amplitude oscillations which can (locally and occasionally) cause $\rho(x, t)$ to vanish. As a consequence, at all those points (hereinafter called space-time defects or phase singularities) the global phase of the field $\Phi \equiv \arctan\left[\frac{\mathbf{Im}(A)}{\mathbf{Re}(A)}\right]$ shows a singularity.

All simulations presented here were performed with a Crank-Nicholson, Adams-Bashforth scheme which is second order in space and time (Press *et al.*, 1992), with a time step $\delta t = 10^{-2}$ and a grid size $\delta x = 0.25$. Three system size ($L = 100, 10^3, 5\,10^3$) have been considered, and in all cases periodic boundary conditions $[A(0, t) = A(L, t)]$ have been imposed.

(*a*) *Dynamics Characterization*

A first interesting parameter characterizing the CGLE dynamics is the defect density. By adding up all defects appearing during a numerical simulation, one can define

$$n_D = \frac{N_{def}}{LT}, \tag{2.5}$$

where L is the system size and T is the integration time during which the number of phase defects N_{def} is counted. Numerically, phase defects at time t have been counted as those points x_i where the modulus $\rho(x_i, t)$ is smaller than $2.5 * 10^{-2}$ and that are furthermore local minima for the function $\rho(x, t)$.

Figure 2 shows n_D *vs.* the parameter β at $\alpha = 2$ for different system sizes. The quantity n_D is clearly an intensive parameter (from a thermodynamic sense), and is a good indicator for differentiating between AT and PT regime. It is interesting to note, however, that the transition between AT and PT is not sharp and depends of the system size. The complete characterization of this transition is still a question of debate.

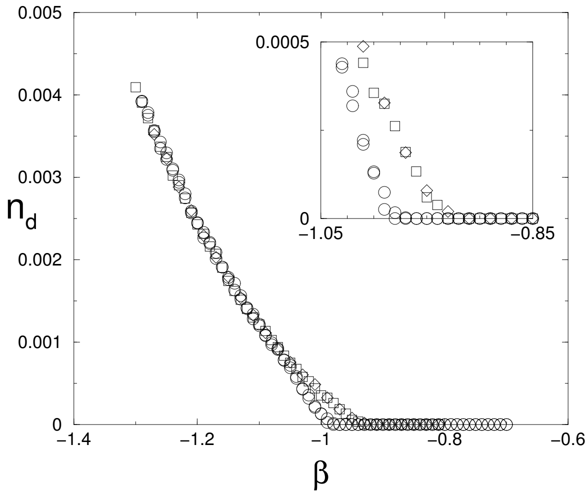

Figure 2. Defect density as a function of β for different system sizes. Open circles, squares and diamonds are for $L = 100, 1000, 5000$, respectively.

A second important parameter is the natural average frequency. Such a frequency is calculated from long numerical simulations of CGLE by averaging in space the unfolded phase ϕ defined in $\mathbb{R}$ rather than in $[0, 2\pi]$. We have:

$$\Omega = \lim_{t \to \infty} \frac{< \phi(x,t) >_x}{t} \tag{2.6}$$

where $< ... >_x$ stands for spatial average.

Figure 3 reports Ω *vs.* the parameter β at $\alpha = 2$. In order to construct Fig. 3, we have integrated the CGLE for a very long simulation time (usually $t_s = 15,000$) after eliminating the transient behavior occurring in the first $t_t = 5,000$. We also have tested the sensibility of the results by choosing different initial random conditions.

It should be emphasized that all initial conditions were chosen to have a zero average phase gradient, because the frequency in the PT regime is highly sensitive to the average phase gradient (Brusch *et al.*, 2001).

A third indicator is the linear spatial auto-correlation function

$$C(\xi) =< \bar{A}(x,t) A(x+\xi,t)) >_t \tag{2.7}$$

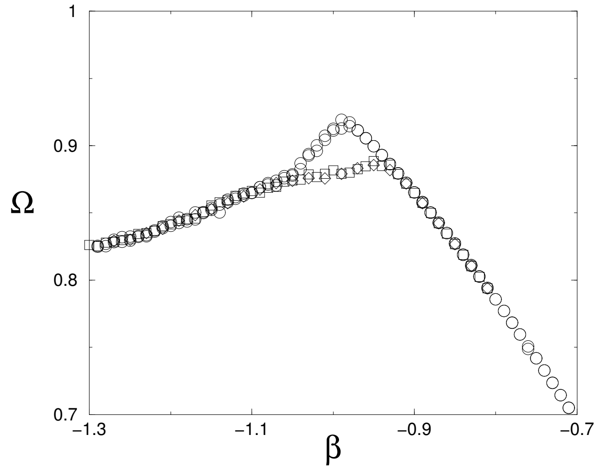

Figure 3. Natural averaged frequency Ω (see text for definition) *vs.* β for $\alpha = 2$. The same symbol convention is used for the system size L as in Fig. 2.

where $< ... >_t$ stands here for a time average. It has been theoretically predicted (Coullet *et al.*, 1989) that the defects have a dynamical role in mediating the shrinking process of ξ. Figure 4 strikingly illustrates this fact for the CGLE. The AT regime (solid line) is for parameters $\alpha = 2$ and $\beta = -1.05$ and the parameters for the PT regime (dashed line) are $\alpha = 2$ and $\beta = -0.87$. The decays to zero are not exponential but we can still define the correlation length as the value of ξ for which $C(\xi) = 1/e$, in doing so we get approximately $\xi = 10.7$ and $\xi = 389$ for the AT and PT regimes, respectively.

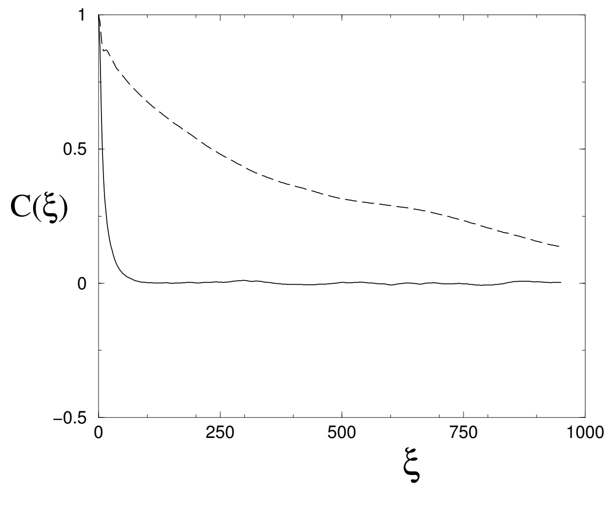

Figure 4. Linear spatial auto-correlation lengths for the AT (solid line) and PT (dashed line) regime of the CGLE (see text for parameters values). The system size L is 5,000.

From our discussion we have learned that the CGLE dynamics can be characterized by some intensive indicators as the density of defects, the natural frequency or the correlation length. With increasing the system extension (L), the values of these three parameters is constant, for system sizes large enough to prevent the dynamics from being affected by any "finite size" effects.

3. Control of the CGLE

After having characterized the dynamics of the CGLE, we will attack the problem of its control. In particular, we will address the issue of whether control can be achieved for a certain number of controllers (extensive case) or rather for a certain density of controllers (intensive case). In this section, we will point out that it is the density rather than the number of controllers that determines control over the spatio-temporal dynamics. For this purpose, we will test a control strategy for two system sizes ($L = 100$ and $L = 5,000$) that differ by a factor fifty.

Let us begin with the problem of controlling space time chaos in the AT regime. For this purpose, we set $\alpha = 2$ and $\beta = -1.05$. In a previous analysis (Boccaletti *et al.*, 1999) we have used a system size of $L = 64$ which is nearly two order of magnitude smaller than the larger one reported here, and have demonstrated that the control of space-time chaos is doable. Control of space time chaos here would imply stabilization of a given unstable periodic pattern out of the AT regime. We therefore select a goal pattern $g(x,t)$, represented by any of the plane wave solutions in Eq.(2.2), which are all unstable in the AT regime.

In order to drive the dynamics to the desired goal pattern we add to the right-hand-side of Eq.(2.1) a perturbative term $U(x,t)$ of the type

$$\begin{aligned} U(x,t) &= 0 \qquad &\text{for } x \neq x_i \\ U(x,t) &= U_i(t) \qquad &\text{for } x = x_i \end{aligned} \tag{3.1}$$

where $i = 1, ..., M$ and $x_i = 1 + (i-1)\nu$ are the positions of M local equally spaced controllers, mutually separated by a distance ν ($x_{i+1} - x_i = \nu$). The controller distance ν will indeed be a crucial parameter in our studies. It indicates in some sense how dense the controllers must be in order to attain the goal dynamics, and we will show that i) such density should be relatively large for the control to be effective and ii) such density is indeed independent of the system size L. In our previous analyses (Boccaletti *et al.*, 1999), the perturbations were selected by using the adaptive algorithm (Boccaletti & Arecchi, 1995). In such a case, however, a full control of the perturbation strength applied to the system is not always guaranteed, and, in some cases, the perturbation can occasionally reach unacceptably large values. This represents a limitation of our previous approach, especially if one wants to apply this scheme on a real experiments. We here will turn to the simpler Pyragas control scheme where the strength of the perturbation K_0 is fixed externally by the operator. The perturbation takes the form

$$U_i(t) = K_0(g(x_i,t) - A(x_i,t)). \tag{3.2}$$

Figure 5 reports the control task of one of the unstable plane wave for $K_0 = 1$ and $\nu = 0.25$ and a system size ($L = 5,000$). The control procedure is effective

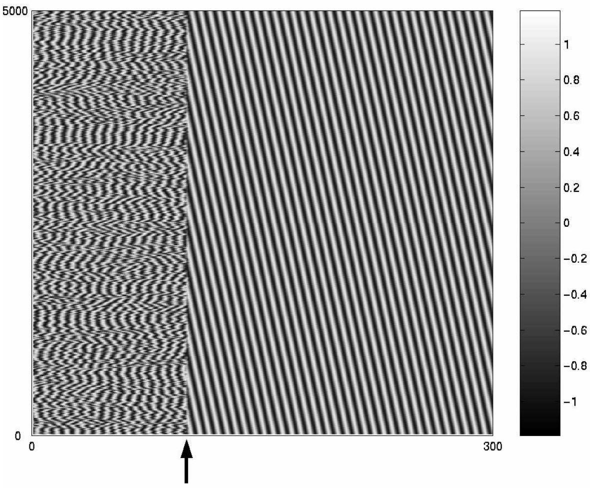

Figure 5. Space (vertical)- time (horizontal) plot of the real part of A in the AT regime ($\beta = -1.05$). Time is increasing from 0 to 300 and the control is switched on at $t = 100$. The parameters for the control are $K_0 = 1$ and $\nu = 0.25$. The goal dynamics is chosen such that the system size $L = 5,000$ contains 10 wavelengths of the desired PWS. The associated frequency $\omega = 1.0495$ is calculated from the dispersion relation Eq.(2.3). The system size L is 5,000.

in the AT regime, and is associated with the suppression of all defects. The arrow indicates the time when the control is switched on.

The control process described above also works for the PT regime, as shown in Fig. 6. In the following, we move to compare quantitatively the difference between the two control processes in the AT and PT regimes and for two different system sizes. Our evidence will indicate that the PT regime is only slightly more easily controllable, for the parameters selected in the present study.

In order to make such quantitative comparison, we monitor the time evolution of the difference between the goal solution and the field A

$$E(t) = \frac{1}{L} \int |A(x,t) - g(x,t)| \, dx \tag{3.3}$$

where the factor $1/L$ accounts for averaging over space. Figure 7 reports the time evolution of $E(t)$ for the AT (solid line) and PT (dashed line) regimes. It is apparent from the figure that the difference between controlling a PT or AT regime is not significant when selecting $K_0 = 0.5$ and $\nu = 0.25$.

In order to gather more information on the control process, we define the transient time τ needed for control as the time at which the error $E(t)$ becomes smaller than a given threshold (in what follows we set the threshold to be 10^{-2}).

This allows us to study the influence on control of the two main parameters used in our scheme, namely the fixed strength of the control K_0 and the distance between two adjacent controllers ν, for the two chosen system sizes $L = 100$ and $L = 5,000$.

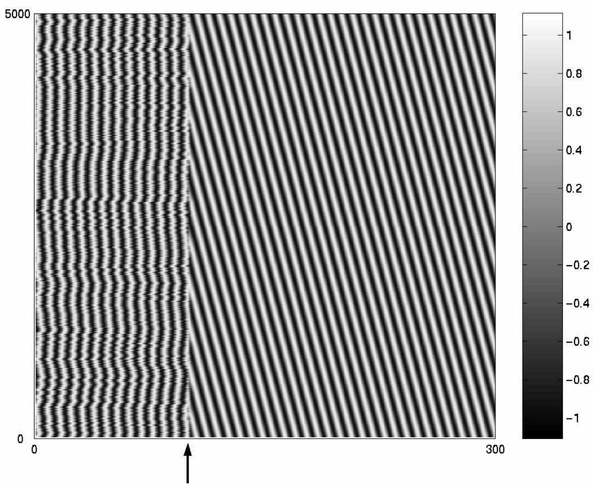

Figure 6. Space (vertical)- time (horizontal) plot of the real part of A in the PT regime ($\beta = -0.87$). Time is increasing from 0 to 300 and the control is switched on at $t = 100$. The parameters for the control are $K_0 = 1$ and $\nu = 0.25$. The goal dynamics is chosen such that the system size $L = 5,000$ contains 10 wavelengths of the desired PWS. The associated frequency $\omega = 0.8695$ is calculated from the dispersion relation Eq.(2.3). The system size L is 5,000.

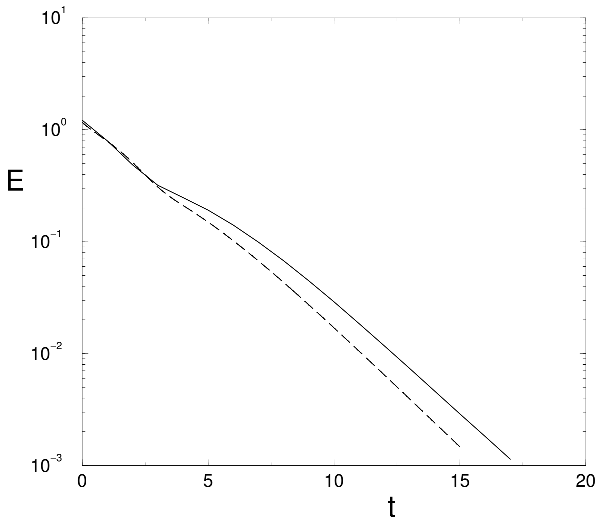

Figure 7. Time evolution of the control error (see text for definition) for the AT (solid line) and PT (dashed line) regimes. The control parameters are $K_0 = 0.5$ and $\nu = 0.25$. The system size L is 5,000.

As one would expect, the transient time τ is an increasing function of ν, at a fixed value of K_0. Furthermore, we observe that there is a threshold for controller density below which the control method fails in stabilizing the PWS for any value of the coupling strength K_0. An example of this behavior is reported in Fig. 8, which shows how τ increases with ν for $K_0 = 1$, for both AT and PT regimes. Figure 8 confirms that the density of controllers is indeed the important quantity that enables control. The two system sizes $L = 100$ and $L = 5,000$ are represented by open and filled symbols, respectively.

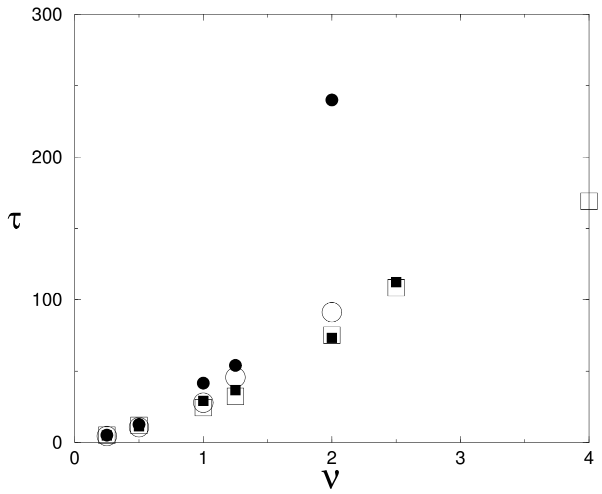

Figure 8. Dependency of the control time τ with the separation of the controllers ν for two different system sizes ($L = 100$ is represented with open symbols and $L = 5,000$ is represented with filled symbols). Squares and Circles are for the control of the PT and AT regimes, respectively. The control parameter $K_0 = 1$ is fixed.

Intuitively, one would also expect τ to be a decreasing function of K_0 at fixed ν, reflecting the fact that an initial choice of a larger control strength helps the system to attain more rapidly the desired goal behavior. Figure 9 confirms this fact by reporting the dependency of the control time τ with the control strength K_0 at fixed density of controllers $\nu = 0.25$ and for the two system sizes ($L = 100$ and $L = 5,000$).

4. Conclusions and Perspectives

In this article, we have reconsidered the problem of controlling a spatio-temporal state generated by a CGLE into an unstable plane wave solution. In the present study, we have considered two different system sizes ($L = 100$ and $L = 5,000$) nearly two order of magnitude apart from each other. Control of spatio-temporal chaos is achieved for sufficient large control strength and density of controllers. It is also interesting to note that the result of Bragard & Boccaletti (2000) concerning the integral behavior of the synchronization is also valid for the case of control. Let us recall that it states that if the distance between the controllers is doubled the strength must be also doubled in order to achieved control in the same time.

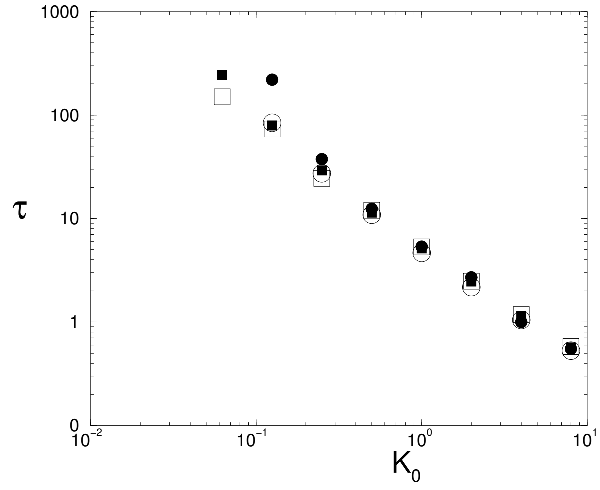

Figure 9. Dependency of the control time τ with the control strength K_0. Symbols have the same meaning as for Fig. 8 The separation between the controllers is fixed to $\nu = 0.25$. Note the logarithmic scales for both axes.

The questions that we leave for further studies are the following: will a further increase in the size of the system eventually compromising the ability of control? In the thermodynamic limit ($L \to \infty$), for instance, one would really need an infinite number of controllers. Apart of being very difficult to realize in practice, one may ask if control is still "stable" in this thermodynamic limit. Another relevant question is whether the selection of equally spaced controllers represents an optimal choice for achieving stabilization of PWS. An answer to this question would result from comparatively testing the effectiveness of different controller positioning functions, or from giving analytical conditions for optimal controller placing. In this context, a promising approach has been proposed that connects control of spatio-temporal chaos with the Floquet control theory (Baba *et al.*, 2002).

Work partly supported by MIUR-FIRB project n. RBNE01CW3M-001. J.B. acknowledges support from MCYT project (Spain) n. BFM2002-02011 (INEFLUID).

References

Aranson, I. & Kramer, L. 2002 The world of the complex Ginzburg-Landau equation. *Rev. Mod. Phys.* **74**, 99–143.

Aranson, I., Levine, H. & Tsimring, L. 1994 Controlling spatio-temporal chaos. *Phys. Rev. Lett.* **72**, 2561–2564.

Baba, N., Amann, A., Schoell, E. & Just, W. 2002 Giant improvement of time-delayed feedback control by spatio-temporal filtering. *Phys. Rev. Lett.* **89**, 074101.

Benkler, E., Kreuzer, M., Neubecker, R. & Tschudi, T. 2000 Experimental Control of Unstable Patterns and Elimination of Spatiotemporal Disorder in Nonlinear Optics, *Phys. Rev. Lett.* **84**, 879-882.

Bleich, M., Hochheiser, D., Moloney, J. & Socolar, E. 1997. Controlling extended systems with spatially filtered, time delayed feedback. *Phys. Rev. E* **55**, 2119–2126.

Boccaletti, S. & Arecchi, F.T. 1995 Adaptive control of chaos. *Europhys. Lett.* **31**, 127–132.

Boccaletti, S., Maza, D., Mancini, H., Genesio, R. & Arecchi, F.T. 1997 Control of Defects and Space-Like Structures in Delayed Dynamical Systems, *Phys. Rev. Lett.* **79**, 5246–5249.

Boccaletti, S., Farini, A. & Arecchi, F.T. 1997b Adaptive Synchronization of Chaos for Secure Communication, *Phys. Rev. E* **55**, 4979-4981.

Boccaletti, S., Bragard, J. & Arecchi, F.T. 1999 Controlling and synchronizing space time chaos. *Phys. Rev. E* **59**, 6574–6578.

Boccaletti, S., Grebogi, C., Lai, Y.-C., Mancini, H. & Maza, D. 2000 The control of chaos: theory and applications. *Physics Report* **329**, 103–197.

Bragard, J. & Boccaletti, S. 2000 Integral behavior for localized synchronization in non-identical extended systems. *Phys. Rev. E* **62**, 6346–6351.

Brusch, L., Torcini, A., van Hecke, M., Zimmermann, M. & Bar, M. 2001 Modulated amplitude waves and defects formation in the one-dimensional complex Ginzburg-Landau equation. *Physica* **D160**, 127–151.

Chate, H. 1994 Spatiotemporal intermittency regimes of the one-dimensional complex Ginzburg-Landau equation. *Nonlinearity* **7**, 185–204.

Coullet, P., Gill, L. & Rocca, F. 1989. Optical vortices. *Opt. Commun.* **73**, 403–408.

Cross, M. & Hohenberg, P. 1993 Pattern formation out of equilibrium. *Rev. Mod. Phys.* **65**, 851–1112.

Cuomo, K. & Oppenheim, A. 1993 Circuit implementation of synchronized chaos with applications to communications. *Phys. Rev. Lett.* **71**, 65–68.

Ditto, W., Rauseo, S. & Spano, M. 1990 Experimental control of chaos. *Phys. Rev. Lett.* **65**, 3211–3214.

Gershenfeld, N. & Grinstein, G. 1995 Entrainment and communication with dissipative pseudorandom dynamics. *Phys. Rev. Lett.* **74**, 5024–5027.

Grigoriev, R., Cross, M. & Schuster, H. 1997 Pinning control of spatiotemporal chaos. *Phys. Rev. Lett.* **79**, 2795–2798.

Hayes, S., Grebogi, C., Ott, E. & Mark, A. 1994 Experimental control of chaos for communication. *Phys. Rev. Lett.* **73**, 1781–1784.

Hochheiser, D., Moloney, J. & Lega, J. 1997 Controlling optical turbulence. *Phys. Rev. A* **55**, R4011–R4014.

Hunt, E. 1991 Stabilizing high-period orbits in a chaotic system: The diode resonators. *Phys. Rev. Lett.* **67**, 1953–1955.

Janiaud, B., Pumir, A., Bensimon, D., Croquette, V., Richter, H. & Kramer, L. 1992 The Eckhaus instability for traveling waves. *Physica* **D55**, 269–286.

Josephson, B. 1962 Possible new effects in superconductive tunnelling. *Phys. Lett.* **1**, 251–253.

Juul Jensen, S., Schwab, M. & Denz, C. 1998 Manipulation, Stabilization, and Control of Pattern Formation Using Fourier Space Filtering, *Phys. Rev. Lett.* **81**, 1614–1617.

Kolodner, P., Slimani, S., Aubry, N. & Lima, R. 1995 Characterization of dispersive chaos and related states of binary-fluid convection. *Physica* **D85**, 165–224.

Kocarev, L. & Parlitz, U. 1995 General approach for chaotic synchronization with applications to communications. *Phys. Rev. Lett.* **74**, 5028–5031.

Kuramoto, Y. & Koga, S. 1981 Turbulized rotating chemical waves. *Prog. Theor. Phys. Suppl.* **66**, 1081–1085.

Leweke, T. & Provansal, M. 1994 Model for the transition in bluff body wakes. *Phys. Rev. Lett.* **72**, 3174–3177.

Lu, W., Yu, D. & Harrison, R. 1996 Control of patterns in spatiotemporal chaos in optics. *Phys. Rev. Lett.* **76**, 3316–3319.

Martin, R., Scroggie, A., Oppo, G.-L. & Firth, W. 1996 Stabilization, selection and tracking of unstable patterns by Fourier space techniques. *Phys. Rev. Lett.* **77**, 4007–4010.

Meucci, R., Gadomski, W., Ciofini, M. & Arecchi, F. 1994 Experimental control of chaos by means of weak parametric perturbations. *Phys. Rev. E* **49**, R2528–2531.

Meucci, R., Ciofini, M. & Abbate, R. 1996 Suppressing chaos in lasers by negative feedback. *Phys. Rev. E* **53**, R5537–R5540.

Montagne, R. & Colet, P. 1997 Nonlinear diffusion control of spatiotemporal chaos in the complex Ginzburg-Landau equation. *Phys. Rev. E* **56**, 4017–4024.

Ott, E., Grebogi, C. & Yorke, J.A. 1990 Controlling chaos. *Phys. Rev. Lett.* **64**, 1196–1199.

Parmananda, P., Hildebrand, M. & Eiswirth, M. 1997 Controlling turbulence in coupled map lattice system using feedback techniques. *Phys. Rev. E* **56**, 239–244.

Pastur, L., Gostiaux, L., Bortolozzo, U., Boccaletti, S., & Ramazza, P.L. 2004 Experimental targeting and control of spatiotemporal chaos in nonlinear optics, *Phys. Rev. Lett* **93**, 063902 (1-4).

Patnaik, B. & Wei, G. 2002 Controlling wake turbulence. *Phys. Rev. Lett.* **88**, 054502.

Peng, J., Ding, E., Ding, M. & Yang, W. 1996 Synchronizing hyperchaos with a scalar transmitted signal. *Phys. Rev. Lett.* **76**, 904–907.

Petrov, V., Gaspar, V., Masere, J. & Showalter, K. 1993 Controlling chaos in the Belousov-Zhabotinsky reaction. *Nature* **361**, 240–243.

Press, W., Teukolsky, S., Vetterling, W. & Flannery, B. 1992 *Numerical recipes in Fortran 90: The art of scientific computing.* Cambridge University Press.

Pyragas, K. 1992 Continuous control of chaos by self-controlling feedback. *Phys. Lett.* **A170**, 421–428.

Roy, R., Murphy, T., Maier, T. Gills, Z. & Hunt, E. 1992 Dynamical control of chaotic laser: Experimental stabilization of globally coupled system. *Phys. Rev. Lett.* **68**, 1259–1262.

Shraiman, B., Pumir, A., van Saarlos, W., Hohenberg, P., Chaté, H. & Holen, M. 1992 Spatiotemporal chaos in the one-dimensional complex Ginzburg-Landau equation. *Physica* **57**, 241–248.

Torcini, A. 1996 Order parameter for the transition from phase to amplitude turbulence. *Phys. Rev. Lett.* **77**, 1047–1050.

Torcini, A., Frauenkron, H. & Grassberger, P. 1997 Studies of phase turbulence in the one-dimensional complex Ginzburg-Landau equation. *Phys. Rev. E* **55**, 5073–5081.